Materials Characterization 128 (2017) 7–13

Contents lists available at ScienceDirect

Materials Characterization

journal homepage: www.elsevier.com/locate/matchar

Heterogeneous nucleation of Al on AlB_2 in Al-7Si alloy

Jiehua Li[a,b,*], Guangyu Yang[b], Fredrik S. Hage[c], Zongning Chen[d], Tongmin Wang[d], Quentin M. Ramasse[c], Peter Schumacher[a,e]

[a] Institute of Casting Research, Montanuniversität Leoben, A-8700 Leoben, Austria
[b] State Key Laboratory of Solidification Processing, Northwestern Polytechnical University, No. 127 Youyi Western Road, Xi'an, 710072, PR China
[c] SuperSTEM Laboratory, SciTech Daresbury Campus, Keckwick Lane, Daresbury WA4 4AD, UK
[d] Key Laboratory of Solidification Control and Digital Preparation Technology, School of Material Science and Engineering, Dalian University of Technology, Dalian 116024, China
[e] Austrian Foundry Research Institute, Leoben, Austria

ARTICLE INFO

Keywords:
Al alloy
Segregation
Heterogeneous nucleation
High angle annular dark field (HAADF)
Electron energy loss spectroscopy (EELS)

ABSTRACT

High angle annular dark field scanning transmission electron microscope imaging and electron energy loss spectroscopy were used to elucidate the heterogeneous nucleation interface of AlB_2 in an Al-7Si alloy. Si particles were observed in the vicinity of a AlB_2 particle, but no significant Si-B-rich layer (such as SiB_6) was observed at the interface between AlB_2 and Al, strongly indicating that the proposed creation of a layer of SiB_6 at the interface between AlB_2 and Al may only be metastable and further transform to other stable phase (*e.g.* Si) during solidification. The solidification path of Al-Si-B alloy was also discussed based on the binary phase diagrams and a ternary Thermo-Calc simulation using the Scheil module in conjunction with the TCAL3 database. These results provide new insight into the heterogeneous nucleation behavior of Al on AlB_2 influenced by solute Si.

1. Introduction

The grain refinement of aluminum alloys through inoculation (*e.g.* Al-Ti-B) has been widely investigated in the foundry industry due to its high efficiency [1]. The addition of an Al-5Ti-1B grain refiner to Al alloys usually produces a reproducible grain refinement. However, for Al-Si-based foundry alloys with high Si concentrations (higher than 3.5 wt%), the performance of the Al–Ti–B grain refiner is negatively affected by so-called Si poisoning [2,3]. Because most important industrial Al-Si alloys contain about 7–10 wt% Si, avoiding or reducing the Si poisoning effect is of great necessity. In previous research, a change of growth mode (cellular to dendritic) as well as an increase of the latent heat release with increasing Si content were suggested as possible mechanisms to explain the drop in refinement efficiency, along with the formation of τ-AlSiTi phase or $TiSi_2$ phases on TiB_2 particles [2]. The so-called edge to edge matching (E2EM) model has also been put forward to explain the Si poisoning mechanism [3]. However, the E2EM model proposes that a Ti_5Si_3 phase should coat the surface of Al_3Ti, rather than TiB_2. Clearly, the precise nucleation mechanism for primary Al in Al-Si alloys is not yet agreed upon in the scientific community, and there is a need to explore ways to reduce or avoid Si poisoning during solidification.

The addition of AlB_2 particles, instead of TiB_2 particles, is one of the possible effective ways to achieve this goal. On the one hand, thanks to the absence of Ti, the formation of an τ-AlSiTi phase can be avoided. However, AlB_2 particles alone cannot effectively refine Al; for this the presence of Si is required [4–9]. Indeed, high Si concentrations has been reported to enhance the grain refinement efficiency of AlB_2 particles [10–12], indicating that the solute Si may interact with AlB_2 in such a way that it unleashes the nucleating potential of AlB_2. This effect has been attributed to the formation of a SiB_6 layer on the AlB_2 surface [12]. However, there is still a lack of an unambiguous understanding of the interface structure and composition of the AlB_2 and Si interface.

In the present work, high angle annular dark field scanning transmission electron microscope (HAADF-STEM) imaging and electron energy loss spectroscopy (EELS) were used to elucidate the heterogeneous nucleation interface of Al and AlB_2 in an Al-7Si alloy, with a special focus on the effect of solute Si on the heterogeneous nucleation of Al on AlB_2.

2. Experimental

Commercial purity (CP) Al (99.8%) and high purity Si (99.97%) were melted in a medium-frequency induction furnace to produce Al–7Si alloys with an addition of B up to 0.2 wt% (all compositions are in wt% unless otherwise specified) *via* an Al–3B master alloy at 780 °C.

* Corresponding author at: Institute of Casting Research, Montanuniversität Leoben, A-8700 Leoben, Austria.
E-mail address: jie-hua.li@hotmail.com (J. Li).

http://dx.doi.org/10.1016/j.matchar.2017.03.029
Received 20 January 2017; Received in revised form 24 February 2017; Accepted 19 March 2017
1044-5803/

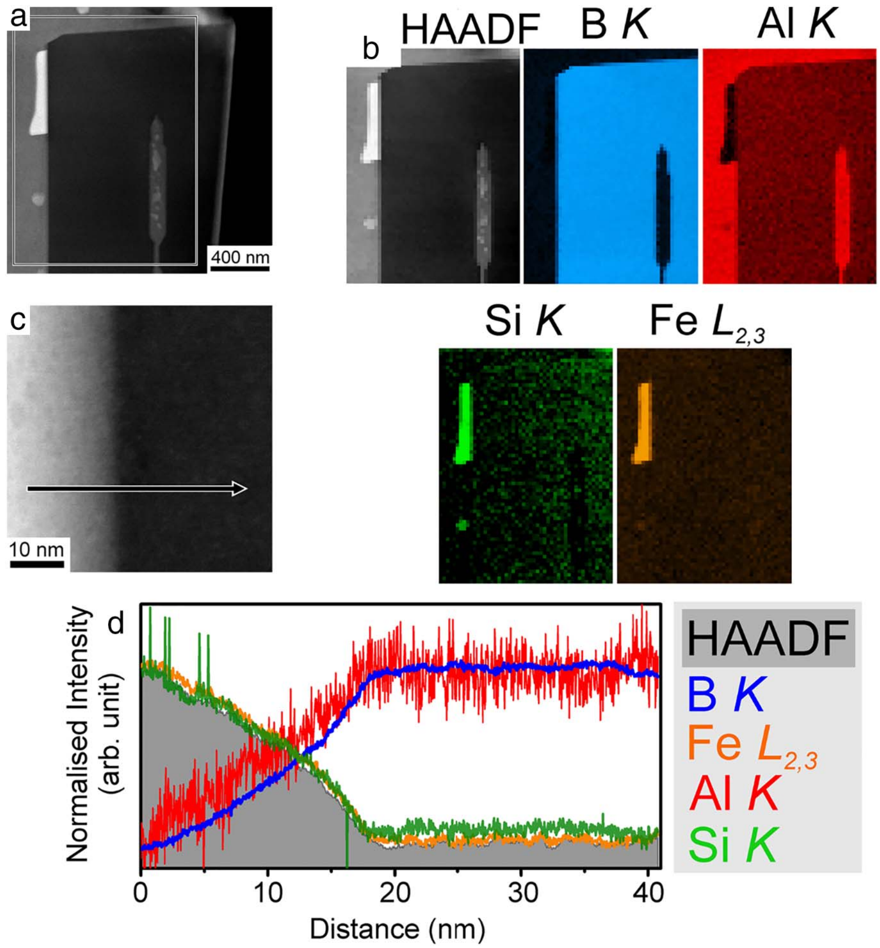

Fig. 1. HAADF STEM images (a, c), EELS maps of B, Al, Si, Fe (b), and a line scan across the interface (d) between AlB_2 and Al, as marked with a black solid arrow in (c) in the Al-7Si-0.2B alloy.

After stirring, the melt was cast into a preheated graphite mold with an average cooling rate of 1.5 K/s at the center of the casting.

Thin foil samples containing AlB_2/Al interfaces were prepared using focused ion beam (FIB) (FEI Helios NanoLab 660). Lamellae were extracted perpendicular to the sample surface using the standard lift-out technique. After initial thinning of the TEM lamellae samples, low energy ion milling at a voltage of 0.2 kV was performed to minimize possible damage induced by Ga + ions and re-deposition of material on the surface of the lamella.

Conventional TEM was performed in an aberration-corrected JEOL-2100F microscope operated at 200 kV. HAADF-STEM imaging and EELS were performed using a Nion UltraSTEM100 aberration corrected dedicated STEM. The microscope was operated at an acceleration voltage of 100 kV and an electron probe convergence semi-angle of 31 mrad, which resulted in an estimated minimum electron probe size of 0.8 Å. The cold field emission gun of the microscope has a native energy spread of 0.35 eV. The HAADF detector collection semi-angle was 83–185 mrad and the spectrometer collection semi-angle was 36 mrad. EELS elemental maps where then created by integrating the EELS signal of each edge (at a nominal edge onset energy): Al *K* (1560 eV), Si *K* (1839 eV), B *K* (188 eV), Fe $L_{2,3}$ (708 eV), over a suitable energy window after subtracting the preceding exponential background fitted with a power law. All EELS edges were identified following reference [13]. EEL spectra were de-noised using Principal Component Analysis (PCA) as implemented in the MSA plugin for [14] for Gatan's Digital Micrograph software. The intensities of the EELS maps were displayed on a false colour scale, so that within each map, a low intensity (black) corresponds to a lower relative concentration, while an increased contrast (colour) corresponds to an increase in (relative) elemental concentration.

3. Results

Fig. 1 shows HAADF STEM images (Fig. 1a, c), EELS maps of B, Al and Si (Fig. 1b), and, a line scan across the interface between AlB_2 and Al in the Al-7Si-0.2B alloy (Fig. 1d), as indicated with a black solid arrow in (Fig. 1c). Two Si-Fe rich particles were observed in the vicinity of the AlB_2 particle. The ratio of Fe/Si is close to 1:1, indicating that the Si-Fe rich particles are very likely to be β-Al_5SiFe phase, which can be further confirmed by further high resolution TEM characterisation (Fig. 2). The presence of Fe can be attributed to the original impurities in the commercial purity Al used raw material. Furthermore, an